# EXPERIMENTAL STATIC CALIBRATION OF AN IMU (INERTIAL MEASUREMENT UNIT) BASED ON MEMS

**Hélio Koiti Kuga, hkk@dem.inpe.br**
**Roberto Vieira da Fonseca Lopes, roberto@dss.inpe.br**
**Walter Einwoegerer, weinwoegerer@gmail.com**
Instituto Nacional de Pesquisas Espaciais - INPE
*CP 515 - São José dos Campos, SP - 12227-010 - Brazil*

***Abstract.*** *This work describes the static alignment of a low cost IMU (inertial measurement unit) based on MEMS (Micro Electro-Mechanical System) technology. A precise 3-axis turn table was used to collect measurements from the accelerometers and gyros. For the case of a static alignment, a non-linear Kalman filter was developed to accomplish in real time the estimates of calibration parameters, in order to minimize the navigation errors. The efficiency and performance of the parameters estimation algorithm were shown to be in accordance with the proposition of error reduction. Shown is also the level of precision as well as the time response of the filter to reach accuracy considered satisfactory for this type of sensor.*

***Keywords****: IMU, static alignment, Non linear Kalman filter, Sigma-Point filter.*

## 1. INTRODUCTION

This work describes the experiment for the static alignment of an IMU (inertial measurement unit), composed of sensors based on MEMS (Micro Electro-Mechanical System) technology. IMU-MEMS are inertial units of low cost and performance that can be considered for low precision applications. The procedures to assemble the IMU in a 3-axis turn table, and to collect data and raw measurements of the accelerometers and gyros are detailed. In a static situation, being the state fully known, this information can be feed to the algorithm for initial parameters calibration. The paper describes the first results that, from the development of an algorithm to initial calibration, makes possible the reduction of errors when IMU-MEMS are used. One tried to identify errors not compensated or controlled acting on these sensors, such as bias, linearity and misalignment, among others. In the experiment it was used a commercial IMU-MEMS (Crossbow IMU400CD), composed of 3 accelerometers and 3 gyros temperature compensated. The set was mounted in a high accuracy Contraves (53M2/30H) 3-axis turn-table, and the data acquisition was established through a serial (RS-232) interface. From the measurements taken and the numerical integration of the differential equations of navigation, the relevant parameters that defined the algorithm to be implemented were evaluated. A Kalman filter was developed to accomplish in real time the estimates of those parameters, in order to minimize the navigation errors. As main conclusion, it can be drawn that the results on the efficiency of the parameters estimation and on the performance of the tested algorithm, were shown to be in accordance with the proposition of error reduction. It is also shown the level of precision, as well as the time response of the filter to reach an accuracy considered satisfactory for this type of sensor.

## 2. EXPERIMENT SETUP

In terms of equipment, the experiment setup used a low cost MEMS (Micro-Electro-Mechanical-System) IMU (Inertial Measurement Unit), a high precision 3-axis turn table, and a PC to process the data.

The commercial IMU-MEMS (Crossbow model IMU-CD400-200) used in the experiment is composed of 3 accelerometers and 3 gyros temperature compensated with digital (RS-232) and analog (12-bit DAC) interface outputs (Crossbow, 2007). This strapdown inertial system provides measurement of linear acceleration and angular rate. The data acquisition was performed through a RS-232 communication serial port, whose protocol is a Crossbow proprietary format. This IMU is a six-degree of freedom measurement system designed to measure linear acceleration along three orthogonal axes and rotation rates around the same three orthogonal axes. Such three accelerometers and three angular rate sensors are capable of responding quickly to translational and rotational motions and provides a complete measurement set from which it is possible to compute the dynamic motion of the system. Its maximum sampling rate is 133Hz configurable. Start-up time to obtain valid data, via serial interface, is less than 1s. The experiment is conducted such that initially the IMU is warmed up to avoid thermal transients during the experiment time span, and the rate sensors zeroed at the first use on the turn-table. The IMU has a label on the face illustrating de IMU coordinate system as shown in Figure 1. With the connector facing you, and the mounting plate down, the axes are defined as X-axis – from face with connector through the IMU, Y-axis – along the face with connector from left to right, Z-axis – along the face with the connector from top to bottom. In terms of attitude, when the axes are initially aligned with the north-east-down directions, the axis are named roll, pitch and yaw axes. Regarding the accelerometers, gravitational acceleration is directed downward and is defined as positive for the Z-axis. For taking measurements, the scaled sensor mode

(Crossbow, 2007) has been used, so the analog sensors were sampled, properly converted to digital data, temperature compensated and scaled to engineering units. IMU measurement data were collected externally through turn table slip rings whose connections implemented the RS-232 interface. Most of the experiment sorted data at sampling rates of 0.1, 1, 20, and 133Hz. Table 1 gives the main specifications of the IMU (Crossbow, 2007).

Table 1 – Specifications of CROSSBOW MEMS-IMU-CD400-200

| **Gyro characteristics** | **Value** | **Accelerometer characteristics** | **value** |
|---|---|---|---|
| Range Roll, Pitch, Yaw ($^o$/sec) | ± 200 | Range X, Y, Z (g) | ± 4 |
| Bias Roll, Pitch, Yaw ($^o$/sec) | < ± 1.0 | Bias X, Y, Z (mg) | < ± 12 |
| Scale Factor Accuracy (%) | < 1 | Factor Accuracy (%) | < 1 |
| Non-Linearity (% FS) | < 0.3 | Non-Linearity (% FS) | < 1 |
| Resolution ($^o$/sec) | < 0.05 | Resolution (mg) | < 0.6 |
| Bandwidth (Hz) | > 25 | Bandwidth (Hz) | > 75 |
| Random Walk ($^o$/hr$^{1/2}$) | < 4.5 | Random Walk (m/s/hr$^{1/2}$) | < 1 |

The IMU MEMS was mounted and tested on the 3-axis turn table CONTRAVES 53M-2 Model, which presents a high dynamic performance and a large payload capability. Precise control and measurement instrumentation is provided by Model 30H Modular Precision Angular Control System (MPACS) where a wide variety of analog and digital interface capabilities are available. Table 2 presents the main specifications of the CONTRAVES 53 M-2 turn table.

Table 2 – Specifications of CONTRAVES 53M-2 three-axis turn table

| **Specification** | **Outer axis** | **Middle axis** | **Inner axis** |
|---|---|---|---|
| Axis Rate, Maximum | 500 degrees/second | 750 degrees/second | 1000 degrees/second |
| Inertia | 115 ft-lb-sec$^2$, max | 25 ft-lb-sec$^2$, max | 3 ft-lb-sec$^2$, max |
| Peak Torque | 600 ft-lbs | 160 ft-lbs | 90 ft-lbs |
| Continuous Stall Torque | 300 ft-lbs | 80 ft-lbs | 45 ft-lbs |
| Peak Acceleration | 4.8 rad/sec$^2$ | 6.4 rad/sec$^2$ | 15 rad/sec$^2$ |
| Position Accuracy | 0.2376 arc sec | 0.8101 arc sec | 0.6346 arc sec |

The three-axis table has been positioned so that all axes are at zero degrees angles. The external axis is pointed northward true and the inner-most axis is zenithal. The WGS-84 geodetic coordinates of the center of the turn-table inner axis were surveyed by a GPS system (23.21132308°S, 314.14082390°E, 641.203m in WGS-84 coordinates). For the experiment, the center of the IMU assembly was positioned at the center of the turn-table, with x-axis pointing northward, platform horizontally aligned, and z-axis nadir pointed, respectively measuring roll, pitch and yaw angle variations.

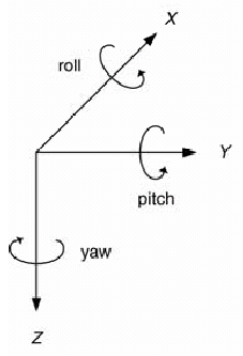


Figure 1 – IMU reference axis

Figure 2 – IMU MEMS mounted on 3-axis turn-table

## 3. NON-LINEAR KALMAN FILTER IMPLEMENTATION

The Kalman filter was developed by Rudolf E. Kalman in 1960 (Brown and Hwang, 1996; Maybeck, 1979; Bierman, 1977). It is an optimal recursive algorithm that estimates the state of a dynamic system from a series of incomplete and noisy measurements. A Kalman filter incorporates all information that can be provided to it, combines the available data measured, regardless of their precision, adds the prior knowledge of the system and of its measuring devices, to produce an estimate of the desired variables in such a manner that the error is minimized statistically along the time, according to an optimality criterium. Because the Kalman filter is a recursive estimator, this means that only the estimated state and covariances from the previous time step and the current measurements are needed to update the estimate for the current state. Starting from a well-known initial state, in the case of a static situation, a Kalman filter could be built to combine all the data available and knowledge of the system dynamics to generate an overall best estimate of not compensated or controlled errors. Due to its characteristics a non-linear Kalman filter was developed to the real time static (motionless) calibration of a MEMS-IMU.

### 3.1. Motion Equations

The differential equations that mechanizes the navigation kinematics (Farrel and Barth, 1998) to determine the IMU's trajectory and attitude motion are given by:

$$\begin{bmatrix} \dot{\varphi} \\ \dot{\lambda} \\ \dot{h} \end{bmatrix} = \begin{bmatrix} \frac{1}{R_n} & 0 & 0 \\ 0 & \frac{1}{R_e \cos\varphi} & 0 \\ 0 & 0 & -1 \end{bmatrix} \begin{bmatrix} V_N \\ V_E \\ V_D \end{bmatrix} \tag{1}$$

$$\begin{bmatrix} \dot{V}_N \\ \dot{V}_E \\ \dot{V}_D \end{bmatrix} = \begin{bmatrix} f_N \\ f_E \\ f_D \end{bmatrix} + \begin{bmatrix} 0 \\ 0 \\ g \end{bmatrix} + \begin{bmatrix} -2\Omega_e V_E \sin(\varphi) + \frac{V_N V_D}{R_n} - \frac{V_E{}^2 \tan(\varphi)}{R_e} \\ 2\Omega_e (V_N \sin(\varphi) + V_D \cos(\varphi)) + \frac{V_E (V_N \tan(\varphi) + V_D)}{R_e} \\ -2\Omega_e V_E \cos(\varphi) - \frac{V_E{}^2}{R_e} - \frac{V_N{}^2}{R_n} \end{bmatrix} \tag{2}$$

$$\begin{bmatrix} \dot{\phi} \\ \dot{\theta} \\ \dot{\psi} \end{bmatrix} = \begin{bmatrix} 1 & \sin\phi\tan\theta & \cos\phi\tan\theta \\ 0 & \cos\phi & -\sin\phi \\ 0 & \frac{\sin\phi}{\cos\theta} & \frac{\cos\phi}{\cos\theta} \end{bmatrix} \left\{ \begin{bmatrix} \bar{p} - b_p \\ \bar{q} - b_q \\ \bar{r} - b_r \end{bmatrix} - R_{n2p} \begin{bmatrix} \Omega_e \cos\varphi + \frac{V_E}{R_e} \\ -\frac{V_N}{R_n} \\ -\Omega_e \sin\varphi - \frac{V_E \tan\varphi}{R_e} \end{bmatrix} \right\} \tag{3}$$

$$\begin{bmatrix} f_N \\ f_E \\ f_D \end{bmatrix} = R_{p2n} \left\{ \begin{bmatrix} \tilde{f}_u \\ \tilde{f}_v \\ \tilde{f}_w \end{bmatrix} - \begin{bmatrix} b_u \\ b_v \\ b_w \end{bmatrix} \right\} \tag{4}$$

where $[\varphi, \lambda, h]$ are the geodetic latitude, longitude, height; $[V_N, V_E, V_D]$ are the velocity components respectively to North, East and Down (NED) directions; $[\phi, \theta, \psi]$ are roll, pitch and yaw angles; $R_e$ is the Earth East radius plus altitude $h$; $R_n$ is the Earth North radius plus altitude $h$; $\boldsymbol{R}_{n2p}$ is the navigation-to-body rotation matrix; $\Omega_e$ is the Earth rotation; $g$ is local gravity calculated taking into account the centripetal force and gravitational attraction; $[p, q, r]$ are the angular rates measured at a given time by the gyros and $[b_p, b_q, b_r]$ are their "biases" respectively; $[f_u, f_v, f_w]$ are the accelerometers measurements at a given time and $[b_u, b_v, b_w]$ are their "biases" respectively; and $[f_E, f_N, f_D]$ are the accelerometers measurements corrected to ECEF coordinate frame. If one wishes to estimate also the biases of the accelerometers and gyros, in its simplest form, they can be modeled as stepwise constants:

$$\begin{aligned} \dot{\boldsymbol{b}}_a &= 0, \\ \dot{\boldsymbol{b}}_g &= 0, \end{aligned} \tag{5}$$

with $\boldsymbol{b}_a \equiv \begin{pmatrix} b_u & b_v & b_w \end{pmatrix}$ and $\boldsymbol{b}_g \equiv \begin{pmatrix} b_p & b_q & b_r \end{pmatrix}$ being the biases of the accelerometers and gyros respectively, augmenting the state from 9 to 15 elements.

When required, the Jacobian (partial derivatives) matrix corresponding to the system of differential equations (1), (2) and (3) is quite complex (Farrel and Barth, 1998) and should be evaluated stepwise, because it changes continuously as a function of position, velocity and attitude of the vehicle:

$$F = \begin{bmatrix} 0 & 0 & \frac{-V_N}{R_a^2} & \frac{1}{R_a} & 0 & 0 & 0 & 0 & 0 \\ \frac{V_E \tan(\varphi)}{R_a \cos(\varphi)} & 0 & \frac{-V_E}{R_a^2 \cos(\varphi)} & 0 & \frac{1}{R_a \cos(\varphi)} & 0 & 0 & 0 & 0 \\ 0 & 0 & 0 & 0 & 0 & -1 & 0 & 0 & 0 \\ F_{41} & 0 & F_{43} & \frac{V_D}{R_a} & 2\omega_D & \frac{V_N}{R_a} & 0 & f_D & -f_E \\ F_{51} & 0 & F_{53} & -(\omega_D + \Omega_D) & F_{55} & \omega_N + \Omega_N & -f_D & 0 & f_N \\ -2V_E\Omega_D & 0 & F_{63} & \frac{-2V_N}{R_a} & -2\omega_N & 0 & f_E & -f_N & 0 \\ -\Omega_D & 0 & \frac{V_E}{R_a^2} & 0 & \frac{-1}{R_a} & 0 & 0 & \omega_D & -\omega_E \\ 0 & 0 & \frac{-V_N}{R_a^2} & \frac{1}{R_a} & 0 & 0 & -\omega_D & 0 & \omega_N \\ \Omega_N + \frac{V_E}{R_a \cos(\varphi)^2} & 0 & \frac{-V_E \tan(\varphi)}{R_a^2} & 0 & \frac{\tan(\varphi)}{R_a} & 0 & \omega_E & -\omega_N & 0 \end{bmatrix} \tag{6}$$

where:

$$\Omega_N = \Omega_e \cos(\varphi)$$
$$\Omega_D = -\Omega_e \sin(\varphi)$$
$$\omega_N = \Omega_N + \frac{V_E}{R_a}$$
$$\omega_E = \frac{-V_N}{R_a}$$
$$\omega_D = \Omega_D + \frac{-V_E \tan(\varphi)}{R_a}$$
$$R_a = \sqrt{(R_n - h).(R_e - h)}$$

$$F_{41} = -2\Omega_N V_E - \frac{V_E{}^2}{R_a \cos^2(\varphi)}$$
$$F_{43} = \frac{V_E{}^2 \tan(\varphi) - V_N V_D}{R_a^2}$$
$$F_{51} = 2(\Omega_N V_N + \Omega_D V_D) + \frac{V_E V_N}{R_a \cos^2(\varphi)}$$
$$F_{53} = -\frac{V_E(V_N \tan(\varphi) + V_D)}{R_a^2}$$
$$F_{55} = \frac{V_N \tan(\varphi) + V_D}{R_a}$$
$$F_{63} = \frac{V_E{}^2 + V_N{}^2}{R_a^2} - 2\frac{g}{R_a}$$

### 3.2. The "conventional" Extended Kalman Filter algorithm

The Kalman filter estimates two variables: $\boldsymbol{x}$, the estimate of the state at time $k$; and $\boldsymbol{P}$, the error covariance matrix, a measure of the estimated accuracy on the state estimate. The Kalman filter has a cycle with two distinct phases: Prediction (time update) and Correction (measurement update). The prediction phase uses the estimate from the previous time step to produce a predicted estimate of the current state. In the correction phase, measurement information from the current time step is processed to refine the predictions and at the end, to arrive at a new, more accurate corrected estimate. Herein the state vector is composed of a minimum set of 15 elements, defined by $\boldsymbol{x} \equiv \begin{pmatrix} x, y, z, \dot{x}, \dot{y}, \dot{z}, \varphi, \theta, \psi, \boldsymbol{b}_a, \boldsymbol{b}_g \end{pmatrix}$, whose stochastic dynamical system, in generic form, is driven by:

$$\dot{x} = f(x) + G\omega \tag{7}$$

where $\boldsymbol{\omega}$ is white noise, and is present explicitly in equations (2), (3), and (5). The majority of the choices to solve a non-linear problem are the "conventional" extended Kalman filter (Maybeck, 1979), which is stated in what follows. In the prediction phase, the state may be obtained by integration of the differential equations (1)-(3) and (5):

$$\dot{\bar{x}} = f(\bar{x}), \tag{8}$$

with initial condition $\bar{x}_{k-1} = \hat{x}_{k-1}$, where $\boldsymbol{f}$ in a non-linear vector function representing the right side of (1) to (3). The covariance can be predicted by:

$$\dot{\bar{P}} = F\bar{P} + \bar{P}F^T + GQG^T \tag{9}$$

with initial condition $\bar{P}_{k-1} = \hat{P}_{k-1}$, and where $\boldsymbol{Q}$ is the noise covariance matrix of the dynamical noise, i.e., $E\left[\boldsymbol{\omega\omega^T}\right] = \boldsymbol{Q}$. Notice the need of evaluating the Jacobian matrix $\boldsymbol{F}$, equation (6), in the matrix differential equation (9), apart from the fact that $\boldsymbol{F}$ is a function of time varying $\boldsymbol{x}$.

The correction phase of the Kalman filter is implemented by:

$$\begin{aligned} K_k &= \bar{P}_k H_k^t \left(H_k \bar{P}_k H_k^t + R_k\right)^{-1} \\ \hat{P}_k &= \bar{P}_k H_k^t (I - K_k H_k)\bar{P}_k \\ \hat{x}_k &= \bar{x}_k + K_k\left[y_k - h_k(\bar{x}_k)\right] \end{aligned} \tag{10}$$

with $H_k \equiv \left[\frac{\partial h_k}{\partial x}\right]_{x=\bar{x}_k}$. In the case of a static situation, the states representing position, velocity and attitude are constant, with position being the WGS-84 geodetic coordinates of the turn table center (see values in section 2), and velocity and attitude values are all null (the MEMS gyros are not able to measure the Earth rotation). Therefore these values, and respective standard deviations can be fed back to correction cycle, equation (10), of the Kalman filter, working as measurements to the problem. In this case, the sensitivity matrix $\boldsymbol{H}$ is the identity matrix with respect to the states $(x, y, z, \dot{x}, \dot{y}, \dot{z}, \varphi, \theta, \psi)$, which makes linear and trivially amenable the implementation of the Kalman filter correction phase.

### 3.2. Sigma-Point Kalman filter

The conventional non linear filters, like the extended Kalman filter, may yield a poor performance in view of problems inherent to non-linear systems, mainly due to the following assumptions:

- Linearization as a good approximation of the (dynamics and measurements) processes;
- Processes assumed gaussian even for highly non linear problems;
- Normally only the mean (first moment) is predicted non-linearly, whereas the covariance is linearized.

Another option is the Kalman filter named Sigma-Point (or "Unscented") Kalman Filter (SPKF or UKF), which uses sampling techniques (Monte Carlo like) to obtain a minimum set of samples, the sigma-points, around the mean (Julier and Uhlmann, 1997, 2004; Julier et al., 2000), which is still representative of the non-linear system. Indeed the method tries to obtain information about the primary moments (mean, covariance, third central moment or skew, and fourth moment or kurtosis) from few samples chosen criteriously. Afterwards, the selected samples, the sigma-points, are non-linearly predicted so as to compute the covariance from the predicted sigma-points (Julier et al., 2000). With this approach the Jacobian matrix $\boldsymbol{F}$ does not need to be evaluated, which becomes an asset using the SPKF for this particular problem. Therefore the SPKF approach is applied only to the prediction phase of the Kalman filter.

Defining $n$ as the size of the state vector to be estimated, one generates a set of $2n+1$ sigma-points by:

$$\hat{\boldsymbol{\chi}}_{k-1}^{o} = \hat{\boldsymbol{x}}_{k-1}$$
$$\hat{\boldsymbol{\chi}}_{k-1}^{i} = \hat{\boldsymbol{x}}_{k-1} + \left(\sqrt{(n+\kappa)\hat{\boldsymbol{P}}_{k-1}}\right)_i, \; i = 1,\ldots,n \tag{11}$$
$$\hat{\boldsymbol{\chi}}_{k-1}^{i+n} = \hat{\boldsymbol{x}}_{k-1} - \left(\sqrt{(n+\kappa)\hat{\boldsymbol{P}}_{k-1}}\right)_i, \; i = 1,\ldots,n$$

where $\left(\sqrt{(n+\kappa)\hat{\boldsymbol{P}}_{k-1}}\right)_i$ is the i-th row or column of the square root of matrix $(n+\kappa)\hat{\boldsymbol{P}}_{k-1}$, and the factor $\kappa$ is chosen to scale the moments higher than 3. If $(n+\kappa) = 3$, it is also possible to scale some of the fourth order moments when $\boldsymbol{x}$ is gaussian. The weigths for computing the predicted mean and covariance are given by:

$$W^{o} = \kappa/(n+\kappa)$$
$$W^{i} = 1/(2n+2\kappa), \; i = 1,\ldots,n \tag{12}$$
$$W^{i+n} = 1/(2n+2\kappa), \; i = 1,\ldots,n$$

and the prediction phase of the SPKF is implemented through the integration of equations (1)-(3), (5), for each sigma-point:

$$\dot{\chi}_{i,k+1} = \boldsymbol{f}(\chi_{i,k}). \tag{13}$$

The predicted state mean and covariance are then computed by:

$$\hat{\boldsymbol{x}}_{k+1}^{-} = \sum_{i=0}^{2n} W^{i} \boldsymbol{\chi}_{i,k+1} \tag{14}$$

$$\boldsymbol{P}_{k+1}^{-} = \sum_{i=0}^{2n} W^{i} \left[\boldsymbol{\chi}_{i,k+1} - \hat{\boldsymbol{x}}_{k+1}^{-}\right]\left[\boldsymbol{\chi}_{i,k+1} - \hat{\boldsymbol{x}}_{k+1}^{-}\right]^{T} \tag{15}$$

using the weights according to equation (12).

## 4. SIMULATIONS

The measurement noise variances of the position, velocity, and attitude measurements, used in the developed SPKF, correspond to 10m in horizontal coordinates and 30m in the vertical coordinate, 0.1m/s for velocity components, and 0.1° for the roll and pitch angles and 0.5° for the yaw angle. Such values are typical for GPS measured position and velocity coordinates (Misra and Per Enge, 2001). As far as attitude angles are concerned, the yaw angle was considered less observable in practice. The test cases comprised two sets of data collected statically, i.e., turn table leveled and IMU-MEMS still (fixed and aligned to NED directions) at sampling rates of 20Hz and 133Hz. For typical test cases the biases (and RMS) of accelerometers and gyros converged quickly as shown in Figures 3 and 4.

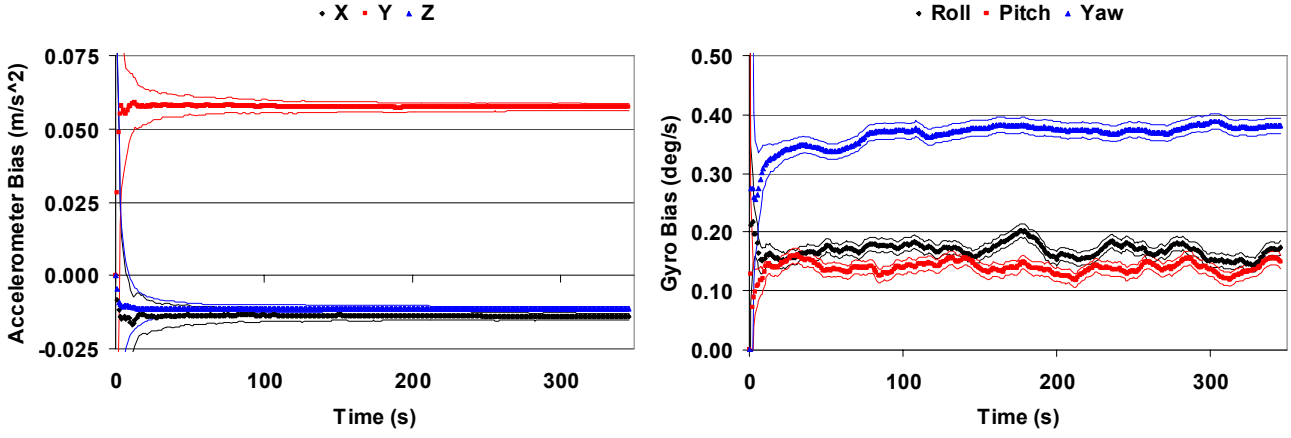


Fig. 3 – Biases of accelerometers and gyros at 20 Hz sampling rate

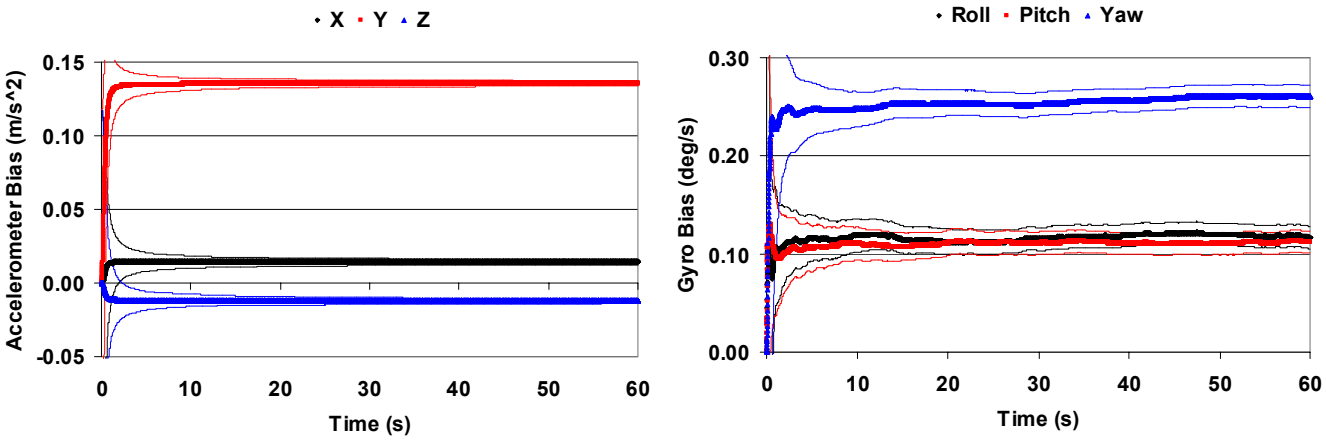


Fig. 4 – Biases of accelerometer and gyro at 133Hz sampling rate

From the figures, it is seen that to attain convergence closer to the final bias values the SPKF needed less than 10s at 133Hz and less than 50s at 20Hz.

Table 3 tabulates the mean estimates and standard deviations on the SPKF mean estimates. It seems that the accuracy on the estimates are strongly correlated with the sampling rate, that is, the higher the sampling rate, the better the accuracy. Standard deviations from data sampled at 133Hz were one order of magnitude better than the ones at 20Hz.

Table 3 – Error on the SPKF estimates

| **Rate (Hz)** | 20 | 133 |
|---|---|---|
| **Height (m)** = 641.2030 | 641.2033±0.0042 | 641.2032±0.0000 |
| $\mathbf{V_N}$ **(m/s)** = 0 | -0.0008±0.0107 | -0.0000±0.0000 |
| $\mathbf{V_E}$ **(m/s)** = 0 | -0.0003±0.0122 | 0.0001±0.0002 |
| $\mathbf{V_D}$ **(m/s)** = 0 | -0.0003±0.0035 | -0.0001±0.0004 |
| $\phi$ **(º)** = 0 | 0.0002±0.0581 | -0.0000±0.0048 |
| $\theta$ **(º)** = 0 | 0.0016±0.0549 | 0.0001±0.0041 |
| $\psi$ **(º)** = 0 | 0.0274±0.1448 | 0.0033±0.0099 |

## 5. CONCLUSIONS

This work described experiments to obtain static alignment in real time of low cost IMUs. The main infra-structure consisted of a very precise 3-axis turn-table which was held horizontally fixed (leveled) and aligned with the NED (North, East, Down) directions. The IMU-MEMS was then aligned parallel to these directions, and data were collected at two sampling rates of 20Hz and 133Hz. An approach using the sigma-point Kalman filter (SPKF) was developed to process the data which avoided the need of computing the Jacobian matrix and delivered very consistent filter estimates. Results have shown a very quick response of SPKF. Future works involve longer campaigns to assess robustness and tolerance to faults, semi-dynamic alignment where axes of the turn-tables are rotating at constant speed (expecting that the SPKF response is not degraded), as well as cases of dynamical motions (e.g. car) on surveyed paths with geodetic accuracy.

## 6. REFERENCES

Bierman, G. J., 1977, "Factorization Methods for Discrete Sequential Estimation", Academic Press, New York.

Brown, R. G. and Hwang, P. Y. C., 1996, "Introduction to Random Signals and Applied Kalman Filtering", John Wiley & Sons, New York.

Crossbow, 2007, "IMU User's Manual Models IMU300CC, IMU400CC, IMU400CD", Revision B, February 2007, Document 7430-0003-03.

Farrel, J.A. and Barth, M., 1998, “The Global Positioning System and Inertial Navigation”, New York, NY, McGraw-Hill, 340 p.
Julier, S.J. and Uhlmann, J.K., 1997, “A New Extension of thee Kalman Filter for Nonlinear Systems”. International Symposium on Aerospace/Defense Sensing, Simulation and Controls, SPIE, 1997.
Julier, S.J. and Uhlmann, J.K., and Durrant-Whyte, H.F., 2000, “A new method for the nonlinear transformation of means and covariances in filters and estimators”. IEEE Transactions on Automatic Control, Vol. 45, Issue 3, p. 477-482.
Julier, S.J. and Uhlmann, J.K., 2004, “Unscented Filtering and Nonlinear Estimation”. Proceedings of the IEEE, Vol. 92, No. 3.
Maybeck, P. S., 1979, “Stochastic Models, Estimation and Control”, Academic Press, New York.
Misra, P. and Enge, P., 2001, "Global Positioning System: Signals, Measurements and Performance", Ganga-Jamuna Press, Lincoln.

## 7. RESPONSIBILITY NOTICE

The author(s) is (are) the only responsible for the printed material included in this paper.